

# Dynamics of Skeletal Pattern Formation in Developing Chick Limb

Stuart A. Newman and H. L. Frisch

A central question in the analysis of embryonic development is how a field of cells that are competent to diversify along more than one pathway do so in a patterned fashion such that appropriate structures appear in the correct posi-

tion shortly after the limb bud emerges from the body wall at 3 days of incubation, is essentially complete at 7 days of incubation, when all the skeletal anlagen have been laid down. After this, the cartilaginous elements are gradually re-

---

**Summary.** During development of the embryonic chick limb the skeletal pattern is laid out as cartilaginous primordia, which emerge in a proximodistal sequence over a period of 4 days. The differentiation of cartilage is preceded by changes in cellular contacts at specific locations in the precartilaginous mesenchyme. Under realistic assumptions, the biosynthesis and diffusion through the extracellular matrix of a cell surface protein, such as fibronectin, will lead to spatial patterns of this molecule that could be the basis of the emergent primordia. As cellular differentiation proceeds, the size of the mesenchymal diffusion chamber is reduced in discrete steps, leading to sequential reorganizations of the morphogen pattern. The successive patterns correspond to observed rows of skeletal elements, whose emergence, in theory and in practice, depends on the maintenance of a unique boundary condition at the limb bud apex.

---

tions. The developing chick limb bud provides an excellent system for studying this question, because the number of distinct terminal cell types is small and their lineage relationships can be examined in culture (1-3), enough material is available to permit biochemical characterization of putative morphogenetic agents (4, 5), and, most importantly, the macroscopic events of the patterning process in the chick limb bud are among the most thoroughly described of any vertebrate system (6-11).

The chick limb, like other vertebrate limbs, develops from the embryonic body wall as a smooth outcropping of mesenchymal cells covered by a thin layer of ectoderm. The limb bud becomes paddle-shaped and elongated by growth under the direction of an ectodermal thickening, the apical ectodermal ridge (AER) (6), that rims its distal margin. During limb outgrowth the differentiation of cartilage proceeds in a proximodistal direction, giving rise to the skeletal anlagen that show characteristic proximodistal, anteroposterior, and dorsoventral polarities (6, 11) (Fig. 1). The patterning process, which begins

placed by bone as the patterned limb continues to increase in size.

Although the mesenchymal cells comprising the early limb bud mesoderm appear to constitute a homogeneous population at all levels of microscopic analysis (12-14), it is now known that the potential of these cells to differentiate into muscle or cartilage is regionalized from the earliest stages of limb formation (15, 16). This is a consequence of the fact that the myogenic and chondrogenic precursor populations have separate points of embryonic origin and are distinct cell types that do not mix to any great extent in the mesoblast (17, 18). Thus, in early limb buds, regions of chondrogenic potential are confined to the central "core" of the mesoderm (16, 17), although at 5 days of incubation the limb tip is potentially almost entirely chondrogenic (1).

Among the cells in the chondrogenic lineage of the limb, the available options appear to be cartilage differentiation, and differentiation into fibroblasts of soft connective tissue or cell death (1, 19). The choice of the cartilage option apparently involves changes in cellular contacts among the progenitor cells, both in

culture and in the developing limb itself (1, 13, 14). This is reflected at the macroscopic level in the precartilaginous condensations first described by Fell and Canti in 1934 (20). Chondrogenic cells that are kept from participating in these interactions in culture, and conceivably in situ, differentiate into fibroblasts or die off (1, 21). It is therefore reasonable to suggest that a molecule that encourages cell-to-cell contacts could be responsible for the initiation of chondrogenic foci in tissue capable of forming cartilage. The problem of pattern formation could then be posed as finding a dynamical scheme by which this molecule could be distributed in appropriate concentrations at appropriate places and times, providing the basis for the emergent skeleton of the limb.

In this article we propose such a scheme. Since the proximodistal polarity of the skeletal elements and the order of their emergence are the most striking aspects of vertebrate limb development, we have concentrated on reproducing these features. Nevertheless, the more subtle anteroposterior and dorsoventral polarities of the limb can also be accommodated within our model with relatively straightforward modifications. The model outlined here has affinities to that of Turing (22), who first recognized that coupling chemical reactions to diffusion can lead to stable, spatially heterogeneous patterns of chemical concentration. We have also been influenced by the analysis of *Drosophila* embryogenesis put forward by Kauffman *et al.* (23), in which Turing's theory was extended to account for pattern succession attendant on growth.

## General Features of the Model

For mathematical convenience we have treated the limb bud, which actually has an oval cross section in the plane perpendicular to the proximodistal axis, as a parallelepiped with a rectangular cross section. Figure 2 shows a drawing of a chick wing bud at 5 days of incubation, alongside our schematization. The limb changes slowly between 3 and 7 days of incubation, adding successive skeletal elements proximodistally, as it increases in size almost exclusively along what we have termed the *z* axis. The wing bud, which is about 0.7 milli-

---

Dr. Newman was an assistant professor in the Department of Biological Sciences, State University of New York, Albany 12222, and is now an associate professor in the Department of Anatomy, New York Medical College, Valhalla 10595. Dr. Frisch is a professor in the Departments of Chemistry and Physics, State University of New York, Albany.

meter in length on day 4 just before the first skeletal element becomes evident, is roughly 5 millimeters in length on day 7, when the skeletal pattern is essentially complete.

We have represented mathematically the following hypothetical situation: A macromolecule, termed M, is loosely bound to the surfaces of the precartilaginous and pre-muscle mesenchymal cells that produce it. This molecule is presumed to be necessary for the formation of contacts between cells competent to differentiate into cartilage. When a critical concentration of M above an initial spatially homogeneous value is exceeded in a particular vicinity, a precartilaginous condensation begins to be formed there. The concentration of M is kept at a constant high level at the AER-mesenchyme interface by its greater production there, but is subject to change at each point in the tissue through a combination of its synthesis and breakdown by the cells and its diffusion through the extracellular matrix. A spatial distribution of the concentration of M is thereby created, with M exceeding the threshold and triggering cartilage differentiation only at specific positions. Regions where M falls below the critical value we will identify with areas of nonchondrogenesis or of cell death (19, 24).

The processes just outlined are presumed to occur in a diffusion chamber consisting of the extracellular matrix [mainly a dilute hyaluronate gel (25)] of the precartilaginous and pre-muscle mesenchyme. This chamber enlarges through the replication of the mesenchymal cells and contracts through the recruitment of cells into muscle and cartilage. This recruitment will be shown to occur at the proximal end of the chamber during most of the pattern-forming process. Therefore the chamber, which initially consists of the entire limb mesoblast, is ultimately confined to the distal tip of the growing limb. As such, it can be identified with the relatively undifferentiated subridge region first described by Saunders (6) and further characterized by Searls (12). This region is similar to what has been termed the progress zone by Summerbell *et al.* (26) or the apical zone by Saunders *et al.* (27).

Our results are based on a simple reaction-diffusion scheme, governed by the steady-state equation for diffusion chambers of discrete size

$$D\nabla^2 c + rc = 0 \quad (1)$$

where  $c$  is related to the displacement of the concentration of M from a spatially homogeneous transient value,  $D$  is the diffusion coefficient of M in the extra-

cellular matrix, and  $r$  is a linearized rate constant for biosynthesis. This equation, under the assumption of appropriate boundary conditions, admits of solutions that are standing waves of the concentration of M along the "anteroposterior" and "dorsoventral" axes of the model limb bud. When solutions are chosen that accord with the real physical dimensions of the limb bud and the actual time scale on which changes occur, it is seen that the number of concentration maxima, and therefore the number of chondrogenic foci, formed along the anteroposterior axis changes discontinuously in a way that depends on the proximodistal length of the diffusion chamber. The shorter the chamber along the latter axis, the larger the number of parallel elements formed along the former axis. In particular, if the contraction of the subridge region occurs in abrupt jumps as differentiation proceeds, as appears to be the case (10), the follow-

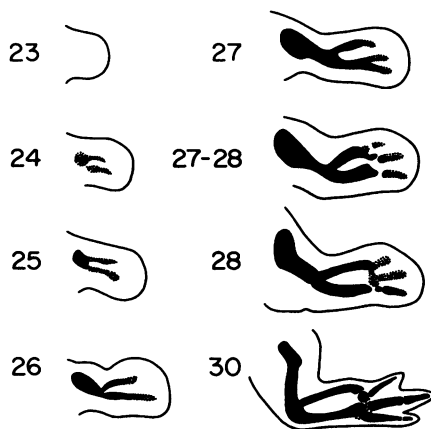


Fig. 1. Progress of chondrogenesis in the chick wing bud between 4 and 7 days of incubation. Solid black regions represent definitive cartilage; stippled areas represent early cartilage. Stages are those of Hamburger and Hamilton (33). Areas of early cartilage are foreshadowed by regions of changed intercellular contact, which occur approximately 12 hours earlier (13). These drawings are based on whole mount photographs of Summerbell (10) and histological studies of Hinchliffe and Ede (39).

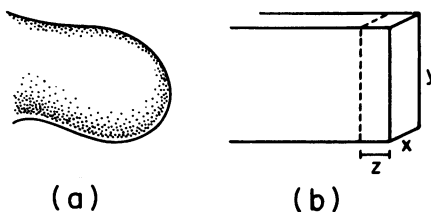


Fig. 2. (a) Drawing of a 5-day wing bud. (b) Schematic representation of wing bud with axes of distal "diffusion chamber" indicated. The  $x$ ,  $y$ , and  $z$  axes of the representation correspond to the dorsoventral, anteroposterior, and proximodistal axes of the limb, respectively.

ing result is obtained: A "humerus," then a "radius" and "ulna," and finally a set of "digits" succeed each other in a proximodistal direction, in a manner that depends critically on the maintenance of a special boundary value at the model limb's distal tip.

### The Saunders Number

The set of solutions to Eq. 1 that we have arrived at (see Appendix) is given by the product of the expressions

$$X(x) = \sin \frac{m_x \pi x}{l_x}, \quad m_x = 1, 2, \dots \quad (2)$$

$$Y(y) = \sin \frac{m_y \pi y}{l_y}, \quad m_y = 1, 2, \dots \quad (3)$$

$$Z(z) = c_0 e^{\lambda z} \quad (4)$$

In the expressions for  $X(x)$  and  $Y(y)$  the  $l_x$  and  $l_y$  in the denominator of the arguments are the constant lengths along the dorsoventral and anteroposterior axes, respectively. The  $\lambda$  in the expression for  $Z(z)$  is related to  $d$ , the proximodistal length of the diffusion chamber, which will take on discrete values as proximal differentiation occurs [see (10) and next section]. The product of these three expressions

$$X(x)Y(y)Z(z)$$

is equal to  $c$ , which is the adjusted displacement of the concentration of M from a spatially homogeneous transient value characteristic of the mesenchyme before the initiation of limb outgrowth (see Appendix).

The relation between the permissible joint values of the arguments of Eqs. 2 to 4 and the reaction and diffusion constants of the system is given by

$$\frac{r l_y^2}{\pi^2 D} \equiv S = \frac{m_x^2}{(l_x/l_y)^2} + m_y^2 - \frac{\lambda^2 l_y^2}{\pi^2} \quad (5)$$

which is derived from Eq. A12 in the Appendix. We refer to the number  $S$  as the Saunders number, after the discoverer of the proximodistal sequence of limb skeletal pattern formation (6).

We will now estimate an order of magnitude for the value of  $S$ . Diffusion coefficients for large molecules in a dilute hyaluronate gel, such as that of the mesenchymal extracellular matrix, would be expected to be somewhat smaller than those in water (28). Since we believe that fibronectin, a large, adhesion-producing cell surface protein found in precartilaginous mesenchyme (5, 29), satisfies the desired properties of molecule M in our formal analysis (see below), we estimate the value of  $D$  in Eq. 5 to be of the order of

$2 \times 10^{-7}$  square centimeter per second, which is about two-thirds the value of the diffusion coefficient in water for a protein of the molecular weight of the fibronectin dimer ( $4.4 \times 10^5$ ) (29, 30). An average measured value of  $l_y$  for the chick wing bud is  $1.4 \times 10^{-1}$  cm (8), so that  $l_y^2$  is  $2 \times 10^{-2}$  cm<sup>2</sup>. The square of  $\pi$  is about 10, and  $r$ , which can be considered as the inverse of the characteristic relaxation time of the pattern-forming process, in which detectable changes take place from hour to hour, is of the order of  $6 \times 10^{-4}$  sec<sup>-1</sup>. These figures set a physically acceptable value for  $S$  at roughly 6.

The maintenance of the value of  $S$  at the approximate magnitude estimated above as the diffusion chamber decreases in size will determine the sequence and spacing of successive concentration wave forms in the growing limb bud, as well as the particular axis along which new modes emerge.

We will now provide estimates for the values of the physical parameters on the right-hand side of Eq. 5. Average values for the quantities  $l_x$  and  $l_y$  of 0.4 and 1.4 mm, respectively, are available from the work of Stark and Searls (8). The values of the chamber length  $d$  when the various skeletal elements are laid down can be inferred from measurements by Searls (12), Stark and Searls (8), and Summerbell (10). These values decline in a discrete fashion from a maximum of about 0.7 mm. The consequence of this will be discussed in succeeding sections. Finally, the choice of a value for  $\lambda$  will determine directly the relation between chamber size and mode number on the right-hand side of Eq. 5, given that the left-hand side is constant. The physical meaning of  $\lambda$ , which can be surmised from Eq. 4 and Fig. 3a, is that it sets the

ratio of the maximum permitted values of  $c$  at the distal and proximal faces of the diffusion chamber. There are, of course, no experimental values for this ratio, since the existence of M is at present hypothetical. We would, however, prefer a value that does not necessitate too extreme a difference in the concentration displacement at the two ends. Therefore, keeping in mind our lack of information in this matter, while attempting to see whether a physically plausible estimate of this quantity can generate a biologically interesting result, we have taken the value of the adjustable parameter  $\lambda$  as  $4.4/d$ . This choice yields a ratio for the largest proximal and distal values of  $c$  of about 81, with the implication that mechanisms to maintain this precise differential could have arisen through natural selection. If likely molecular candidates for M can be identified, a measurement of this ratio could provide an experimental test of the model.

#### Criteria for the Initiation of Prechondrogenic Condensations

The ability of limb mesenchymal cells to respond to M and enter into prechondrogenic condensations depends on several factors, the most important of which are the cells' developmental history and the absence of any antagonistic factor in their microenvironment. The distinctiveness of the precartilaginous and pre-muscle branches of the mesodermal lineage in the limb was discussed in the introduction, along with the fact that these populations are nonuniformly distributed in the limb bud [see also (15-18)]. Thus, the distribution of supra-threshold concentrations of M relative to chondrogenesis in a particular field of

cells is only one aspect of skeletal pattern determination: it is also necessary to know the distribution of competent cells.

For the present analysis it will suffice to postulate that prospective myogenic regions lie outside an ellipse whose major and minor axes are  $2l_y/3$  and  $2l_x/3$ , respectively, during the formation of the humerus; that they lie outside an ellipse whose major and minor axes are  $6l_y/7$  and  $2l_x/3$ , respectively, during formation of the radius and ulna; and that they are of negligible extent during the formation of the digits (1) (Fig. 4). These are crude estimates (15), but the model is largely insensitive to them. In this analysis we make no attempt to explain the distribution of chondrogenic and myogenic primordia.

We will now introduce one more parameter, a factor that does not enter directly into our dynamical equation (Eq. 1) but, like the estimate of the distribution of myogenic cells, serves to delineate the field of cells competent to chondrify in response to M. Thus we will postulate that the limb apex is the source of a substance that inhibits chondrogenesis in competent cells when its concentration is high. Hyaluronate, for example, has been shown to have just such an effect (4, 31). We assume that this material, which we call I, is initially distributed at a uniformly high level in the mesoblast, and effectively prohibits the precartilaginous cells from responding to any concentration of M. At a critical time in the outgrowth of the limb, a sink for I is established at the proximal end of the diffusion chamber. In relation to our hypothesis that hyaluronate could play the role of I, we draw attention to the fact that the enzyme hyaluronidase makes its abrupt appearance in the developing chick limb immediately before the onset

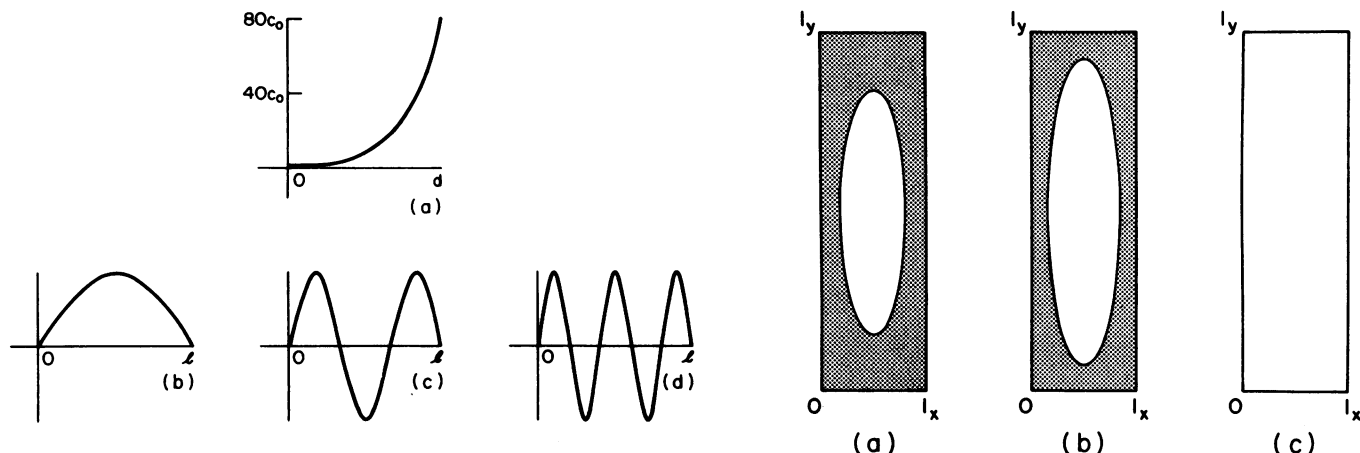


Fig. 3 (left). Graphs of the functions that jointly constitute the solutions of Eq. 1. (a)  $Z(z)$  component of solution; (b)  $X(x)$  or  $Y(y)$  component where  $m = 1$ ; (c)  $X(x)$  or  $Y(y)$  component where  $m = 3$ ; and (d)  $X(x)$  or  $Y(y)$  component where  $m = 5$ . Fig. 4 (right). Schematic representation of potentially chondrogenic (blank) and myogenic (stippled) regions of cross section of wing tip (a) during formation of humerus, (b) during formation of radius and ulna, and (c) during formation of hand.

of chondrogenesis (32). The advent of a sink for I has the effect of changing its spatially uniform concentration into a distribution that decreases linearly from the distal to the proximal ends of the diffusion chamber. This will in turn render a proportion of the cells in the diffusion chamber competent to respond to M. On the basis of the experimentally measured reduction in the size of the "undifferentiated" distal tip as successive elements make their appearance (10), we estimate that roughly one-third of the diffusion chamber becomes responsive in each successive phase of the pattern-forming process. As cartilage differentiation begins, the character of the proximal cells changes (13, 14, 20), their greatly reduced extracellular spaces no longer permitting free diffusion of M. The newly constituted, shorter diffusion chamber is now subject to two transient processes: the reestablishment of the linear gradient of I, brought on by the new production of its sink at the differentiating proximal face of the chamber, and the setting up of a new spatially heterogeneous pattern of M, consistent with the changed dimensions of the chamber. The former process will require more time than the latter if the diffusion coefficient of I is smaller than that of M. If these conditions obtain, any transient pattern of M will have time to decay while the cells are nonpermissive; permissive cells will experience only the time-independent patterns, which will then emerge in the form of centers of cell condensation.

Finally, we must choose the level of M to which competent cells respond by entering into prechondrogenic condensations. If we permit condensations to occur for all positive values of  $c$  larger than a constant  $a$  (see Appendix), we satisfy the reasonable stipulation that no cartilage formation can take place until the spatially uniform initial concentration of M is exceeded.

### Succession of Condensation Modes

#### During Limb Outgrowth

We will now outline the progress of limb development as governed by the reaction-diffusion equation (Eq. 1) subject to the appropriate physical constraints (Eq. 5) and the biological constraints on the availability of chondrogenically competent cells (previous section).

To begin, a linear proximodistal gradient of the substance I ("hyaluronate") is presumed to be established by the appearance of its sink ("hyaluronidase") at the body wall at Hamburger-Hamilton

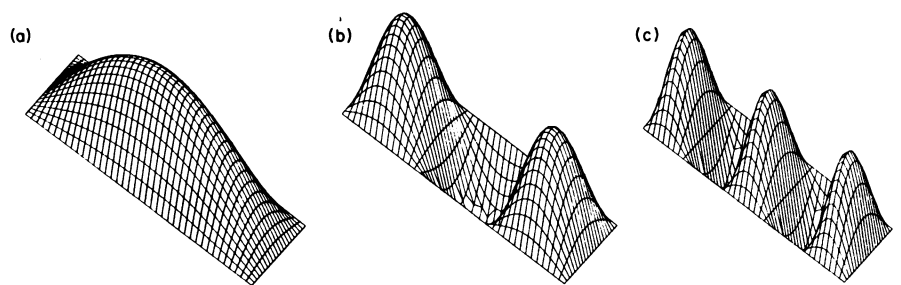


Fig. 5. Product functions  $X(x)Y(y)$ . Functions are those represented in Fig. 3, when (a)  $m_x = 1$ ,  $m_y = 1$ ; (b)  $m_x = 1$ ;  $m_y = 3$ ; (c)  $m_x = 1$ ,  $m_y = 5$ . These product functions indicate the distribution of the substance M on cross sections of the diffusion chamber at various times of development.

stage 21 to 22 (33). At this time (Searls' stage 21-), the wing bud is about 0.7 mm in length (8). Using this value for  $d$  in Eq. 5 and setting  $l_x = 0.4$  mm,  $l_y = 1.4$  mm, and  $\lambda = 4.4/d$ , we arrive at

$$S = 12.5 m_x^2 + m_y^2 - 7.8 \quad (6)$$

If  $m_x$  and  $m_y$  are taken to be 1, this gives a value for  $S$  of 5.7, which is of the order of magnitude previously estimated for the Saunders number.

With this choice for the  $m$ 's, the functional form assumed by both  $X(x)$  and  $Y(y)$  is shown in Fig. 3b. At any level along the  $z$  axis, therefore, the suprathreshold values of  $c$  will be located in a region at the center of the cross section, as specified by the product of  $X(x)$  and  $Y(y)$  (Fig. 5a). The humerus will begin to form in the field of competent cells in the proximal third of the limb, abruptly reducing the size of the diffusion chamber (10, 12).

Searls (12) has estimated that the length of the undifferentiated subridge region at the point where the humerus first becomes evident (his stage 22+) is about 0.5 mm, at which value it remains for the next few stages. This also accords with the estimate of Summerbell (10). Since the cells are now chondrogenically incompetent, no further differentiation can take place until new hyaluronidase is produced at the proximal end of the diffusion chamber, again establishing a linear gradient of I. By the time this occurs, all transients in the concentration of M have had time to decay. The Saunders number must now be calculated with a value of 0.5 mm for  $d$

$$S = 12.5 m_x^2 + m_y^2 - 15.4 \quad (7)$$

The joint values for  $m_x$  and  $m_y$  given above are no longer tenable. Furthermore, the coefficient of the expression in  $m_x$  makes any change in that index disallowed if  $S$  is to remain constant. However, if  $m_y$  is changed to 3, Eq. 7 becomes

$$S = 6.1$$

which is in the acceptable range. Now the functional form assumed by  $Y(y)$  is given by Fig. 3c, and the distribution of suprathreshold values of  $c$  on any cross section is given by the product function in Fig. 5b. The radius and ulna now begin to appear at the proximal end of the diffusion chamber, leading to another abrupt decrease in the value of  $d$  (10).

From the data of Stark and Searls (8), we estimate that it takes until about stage 26 before another set of elements, the wrist, become evident. We interpret this as the lag time needed to set up a new linear gradient of I in the diffusion chamber by the proximally differentiating cells. Using a value for  $d$  of 0.35, which is within the range of experimental values for the tip at this stage (8, 10), we obtain

$$S = 12.5 m_x^2 + m_y^2 - 31.4 \quad (8)$$

which gives an acceptable value of  $S$  only if  $m_y = 5$ . Then Eq. 8 becomes

$$S = 6.1$$

and the functional form of  $Y(y)$  is given by Fig. 3d. The product function in Fig. 5c shows that three cartilaginous elements will now begin to form (34).

The details of the remainder of the developmental process will depend critically on the actual size of the diffusion chamber at the time each new linear gradient of I is set up. Summerbell's data (10) show that in the wing bud there is a recovery in the length  $d$  to its post-radius and ulna size after the wrist forms, probably by cell multiplication. If this is so, our equations would predict the formation of another three-element row, the metacarpals. Subsequent recovery of chamber length during transient periods would continue to preserve the number of elements, while giving rise to joints, such as occur in the digits. Conversely, a reduction in the chamber length that was not reversed would lead to an increase in element number in the more distal

rows—that is, limbs with four or five digits. The process will only cease when the production of I is reduced, conceivably by a fading of ridge activity (35). Then all cells in the chamber become competent to respond to M, exhausting any potential for further addition of elements.

The temporal and spatial pattern of skeletal elements generated by our model is depicted in Fig. 6.

### The *talpid* Polydactylous Mutants of the Chick

At least two recessive lethal mutants exist that exhibit severe aberrations in the pattern of limb chondrogenesis. The most extensively studied have been *talpid*<sup>2</sup> and *talpid*<sup>3</sup>, which develop sufficiently in the homozygous state to permit observation of limb development during the stages under discussion here (36–40) (Fig. 7):

The present model permits one to adduce several critical changes resulting from the mutation that might lead to the anomalies seen in the *talpid* limbs. For instance, the intrinsic responsivity of the precartilaginous cell to the molecule M might be heightened, a possibility we suggested on independent grounds (41). Alternatively, the strength of the signal M might also be increased, through a change in either the distal boundary value of M,  $c_0 e^{\lambda d}$ , or the rate  $R(c)$  by which M is produced and broken down by the cells. The latter possibility is consistent with the finding by Ede and co-workers (40) that the mesenchymal cells of *talpid*<sup>3</sup> have altered adhesivity properties. However, these changes would seem better able to account for the relatively amorphous syndactylous patterns often observed in the *talpid* mutants, in contrast to the strictly polydactylous forms, which are also frequently seen.

Here we would like to suggest an explanation for polydactyly that naturally arises from the particular model we have proposed. In the normal course of development the modes of higher order, corresponding to larger numbers of parallel skeletal elements, are presumed to arise as a decreasing  $d$  forces an increase in  $m_y$  to keep  $S$  constant. In the *talpid* limbs, the length in the  $y$  direction,  $l_y$ , is not constant as it is in normal limbs; rather, it increases with time. In the case of the mutant, Eq. 5 can be rewritten as

$$S' \equiv \frac{r l_x^2}{\pi^2 D} = m_x^2 + \frac{m_y^2 l_x^2}{l_y^2} - \frac{\lambda^2 l_x^2}{\pi^2},$$

$$\lambda = 4.4/d \quad (9)$$

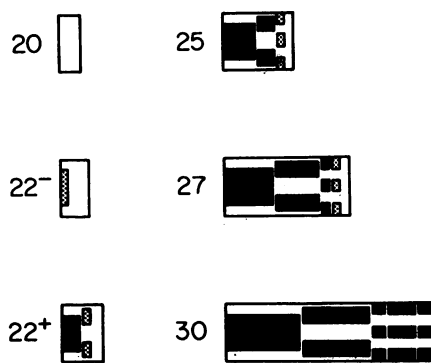


Fig. 6. Patterns of chondrogenesis predicted by the model described in the text at successive stages of development. Elongation of "skeletal elements" is based on empirical measurements (8, 10). Solid black represents cartilage or precartilaginous condensation; stippling represents hypothetical distribution of substance M in competent tissue preceding overt chondrogenesis. Hamburger-Hamilton stages (33) to which the model stages correspond are indicated by numbers.

Here the growth in the variable  $l_y$  has an effect similar to the decrease in  $d$ , as these factors enter into  $S'$  with different signs. Consequently, within the physical constraints common to the normal and mutant limb buds, modes of a higher order than those characteristic of the normal limb will tend to form in the *talpid* limbs, resulting in an increased number of digits dependent on the extent of anomalous expansion in the  $y$  direction (42).

It is, of course, possible that several of the factors discussed in this section might contribute to the *talpid* phenotype. Such factors could even be interrelated; for example, an overproduction of M (perhaps fibronectin) might simultaneously increase the extent of supra-

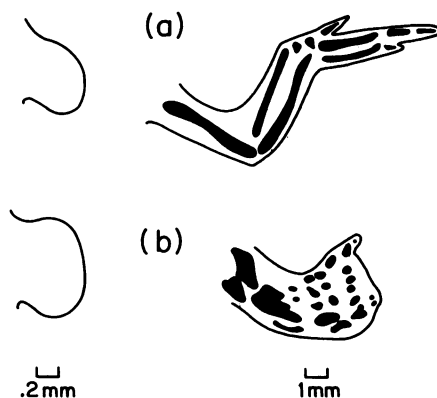


Fig. 7. Shapes of 4-day wing buds (left) and skeletal patterns of 9-day wings (right) of (a) normal and (b) *talpid*<sup>2</sup> embryos. Drawings of 4-day wing buds are based on tracings of Cairns (37). Drawings of 9-day skeletons are based on whole mount photographs of Goetnick and Abbott (38).

threshold levels of the morphogenetic signal, cause the individual cells to be more adhesive, and act so as to expand the diffusion chamber in the  $y$  direction by lengthening the apical ectodermal ridge. We suggest, however, that the aberrantly large number of distinct elements characteristic of the *talpid* phenotype can best be understood by considering the dynamical aspects pointed to by our analysis.

### Conclusions

We have presented a simple model for the generation of the proximodistal sequence of skeletal elements during the development of the chick wing bud. We have not found it necessary to postulate any unusual nonlinear or multicomponent kinetic schemes to generate the discontinuous "switches" in pattern properties that characterize the limb, as well as many other developing systems. Rather, we have relied on a coupling between the metabolism of a single cell surface component and its diffusion through the extracellular matrix to generate standing waves of this putative morphogenetically active material. We have also not needed to posit the growth of random fluctuations to break the spatial symmetry of the morphogen concentration, for the imposition of a nonzero value for  $\beta c_0$  in the solution of our dynamical equation, together with our absorption boundary conditions (see Appendix), forces sinusoidal modes on the spatial distribution of the concentration displacement  $c$ . Although growth of random fluctuations could be an important means of symmetry-breaking in relatively homogeneous systems such as a *Drosophila* egg or imaginal disk (23), it would clearly not be satisfactory in the developing limb bud, which must at some point take its positional bearings from the symmetries already established in the partially developed organism. We have therefore taken advantage of the existence of the AER as a unique factor in limb development (6) and, in terms of the requirements of our model, have attempted to specify the roles that it may play in actual development.

It is notable that the postulated morphogenetic substance M resembles in every respect the peripheral cell surface protein fibronectin (29). The latter is produced by precartilaginous mesenchyme (5), is sloughed off the surfaces of cells into the extracellular matrix (29, 43, 44), is involved in intracellular adhesion (29), and has a molecular weight in its dimeric

form that would give it a diffusion constant of a magnitude required by our model (29). A high concentration of fibronectin at the distal tip of the limb could promote outgrowth by serving as an adhesion substrate for the underlying cells. Significantly, J. Tomasek, working with one of us (S.A.N.), has demonstrated by electron microscopy the presence of an abundance of material resembling fibronectin fibers (44), as well as hyaluronate-like aggregates (45) directly subjacent to the AER of the developing wing bud (46).

We have not speculated on the basis for the distribution of myogenic versus chondrogenic mesenchyme in the limb bud, but we see no reason why the myogenic cells might not differentiate into muscle in response to critical amounts of the same substance M purported to trigger cartilage differentiation in chondrogenic cells. Indeed, values of  $c$  greater than zero occur in peripheral, myogenic regions of the diffusion chamber at all stages (Figs. 4 and 5). This possibility is also in line with our tentative identification of M with fibronectin, since that molecule is transiently found in high concentrations between differentiating myoblasts (47).

Our model might be thought of as giving a physical interpretation to the progress zone idea of Summerbell *et al.* (26), but it differs from the latter in at least one important respect. In our analysis it is not the amount of time spent by a population of cells in the subridge region that determines the proximodistal character of the elements they will become part of, but rather the precise physical dimensions of that region during their residence there. Of course, under normal circumstances, the length of the diffusion chamber will vary inversely with its chronological age, resulting in a general correspondence between proximodistal level and time spent in that region.

The diffusion chamber model accounts well for the distal deficiencies caused by apical ridge removal during limb development (6) as well as the results of tip transplantation experiments that have provided a measure of support for the progress zone idea (26). In addition, the critical role played by the length of the diffusion chamber opens up possibilities for intercalary regulation subsequent to cutting and grafting, for these operations can easily create small alterations in the chamber size. Such regulation has been shown to occur (48), but it is not accounted for by the progress zone concept.

A comment should be made on the for-

mation of the wrist. The possibility that this structure arises during development from a large number of precartilaginous condensations would present problems for the kind of arithmetic progression of modes implied by our model. However, the best recent estimate of the number of wrist and ankle condensations in the chick is three or four (49), as would be expected on the basis of the present analysis.

Many questions remain open. How, within our scheme, can one account for the anteroposterior and dorsoventral polarities that characterize the limb? Must these be introduced by an independent gradient-like system of specification, as suggested by Tickle and co-workers (50) and by Wilby and Ede (51), or can they be accommodated within our model by using more realistic chamber shapes, or even nonuniform circumferential boundary conditions for the system dynamics as might be implied by the clockface model of pattern regulation of French *et al.* (52)? Can the general scheme we have proposed be accommodated to systems such as the amphibian limb, which can regenerate in the adult form (53)? These theoretical questions, as well as experimental problems raised by our model, remain to be resolved.

## Appendix

In this appendix we derive Eq. 1 and its solutions. We postulate that there is a single morphogen M whose concentration is  $C$ . The net rate at which M is produced by the mesenchymal cells is  $R(C)$ . Before the outgrowth of the limb bud begins, M is distributed homogeneously in the prospective limb region of the body wall. At some initial time  $t_0$ , when the spatially homogeneous value of  $C$  is  $C_0$ , the special character of the limb tip is established that fixes its value of  $C$  at  $C_{tip}$  (54). As the model limb bud grows out under the influence of its tip, some M is absorbed at the other bounding surfaces ( $x = 0$ ,  $x = l_x$ ,  $y = 0$ , and  $y = l_y$  in Fig. 2) so that a fixed concentration  $C_b$  is maintained there (55). Inside the model limb,  $C$  is no longer spatially homogeneous, but is described by the complete reaction-diffusion equation for  $t > t_0$

$$\frac{\partial C}{\partial t} = D\nabla^2 C + R(C) \quad (A1)$$

After a short transient, a steady state is achieved for which  $\partial C/\partial t = 0$ ; that is, Eq. A1 simplifies to

$$D\nabla^2 C + R(C) = 0 \quad (A2)$$

We assume that the deviation of  $C$  from  $C_0$ ,  $\hat{c}$ , is sufficiently small that we can expand  $R(C)$  in a Taylor series about  $C_0$

$$\begin{aligned} R(C) &= R(C_0) + \left(\frac{dR}{dC}\right)_{C_0} \hat{c} + O(\hat{c}^2) \\ &\approx R(C_0) + r\hat{c}, \quad r = \frac{1}{\tau} = \left(\frac{dR}{dC}\right)_{C_0} \end{aligned} \quad (A3)$$

where higher-order terms can be neglected. The deviation of  $R$  from  $R(C_0)$  is thus described by a pseudo-first-order rate constant  $r$ , which we take to be positive. The case of negative  $r$  is discussed in (56). The rate constant  $r$  can also be set equal to the reciprocal of the relaxation time  $\tau$  for our reaction.

Let

$$a = \frac{R(C_0)}{r}, \quad c = a + \hat{c} \quad (A4)$$

The number  $a$  is assumed to be small. Now Eq. A3 can be written

$$R(C) = r(a + \hat{c}) = rc \quad (A5)$$

Introducing Eq. A5 into Eq. A2 and recalling that  $C = C_0 + \hat{c} = C_0 - a + c$ , we have

$$D\nabla^2 c + rc = 0, \text{ or}$$

$$\nabla^2 c + \left(\frac{r}{D}\right)c = 0 \quad (A6)$$

which is the same as Eq. 1. The boundary conditions are that  $C_b = C_0 - a$  (that is,  $c = 0$ ) at all bounding surfaces except the tip,  $z = d$ , and the proximal end of the diffusion chamber,  $z = 0$ . On the latter two planes,  $C = C_0 - a + \beta c_0$  (that is,  $c = \beta c_0$ ) and  $C = C_0 - a + c_0$  (that is,  $c = c_0$ ), respectively. The number  $\beta c_0$  is taken sufficiently small that the approximation in Eq. A3 is valid for  $\hat{c} = \beta c_0 - a$ .

We will look for a solution of the form

$$c = X(x) Y(y) Z(z) \quad (A7)$$

Inserting this in Eq. A6 yields

$$\begin{aligned} YZ \frac{d^2 X}{dx^2} + XZ \frac{d^2 Y}{dy^2} + XY \frac{d^2 Z}{dz^2} + \\ \left(\frac{r}{D}\right)XYZ = 0 \end{aligned}$$

Dividing by  $XYZ \neq 0$

$$\begin{aligned} \frac{1}{Z} \left(\frac{d^2 Z}{dz^2}\right) + \frac{r}{D} = \\ -\left(\frac{1}{X} \frac{d^2 X}{dx^2} + \frac{1}{Y} \frac{d^2 Y}{dy^2}\right) \end{aligned} \quad (A8)$$

The left- and right-hand sides, being functions of independent variables, must have a constant value, which we call  $k^2$ .

From the left-hand side of Eq. A8 we obtain

$$\frac{d^2Z}{dz^2} + \left(\frac{r}{D} - k^2\right)Z = 0 \quad (\text{A9})$$

The right-hand side of Eq. A8 yields

$$-\frac{1}{X} \frac{d^2X}{dx^2} = k^2 + \frac{1}{Y} \frac{d^2Y}{dy^2} = k_x^2$$

since, again, both sides are functions of independent variables. Thus

$$\frac{d^2X}{dx^2} + k_x^2X = 0 \quad (\text{A10})$$

and

$$\frac{d^2Y}{dy^2} + (k^2 - k_x^2)Y = 0$$

or

$$\frac{d^2Y}{dy^2} + k_y^2Y = 0 \quad (\text{A11})$$

Then

$$k^2 = k_x^2 + k_y^2$$

From Eq. A9, if  $(r/D) - k^2 = -\lambda^2 < 0$ , then

$$Z(z) = c_0 e^{\lambda z}$$

From Eqs. A10 and A11

$$X(x) = \sin \frac{m_x \pi x}{l_x}, \quad m_x = 1, 2, \dots$$

and

$$Y(y) = \sin \frac{m_y \pi y}{l_y}, \quad m_y = 1, 2, \dots$$

with  $k_x$  and  $k_y$  equal to  $m_x \pi / l_x$  and  $m_y \pi / l_y$ , respectively. The solutions in the  $x$  and  $y$  directions that accord with our boundary conditions are simply integral numbers of half sine waves (57).

Finally, inserting the expressions for  $X(x)$ ,  $Y(y)$ , and  $Z(z)$  into Eq. A8 yields

$$\frac{r}{D} = \frac{m_x^2 \pi^2}{l_x^2} + \frac{m_y^2 \pi^2}{l_y^2} - \lambda^2 \quad (\text{A12})$$

This relationship is central to the analysis we have presented.

#### References and Notes

1. S. A. Newman, in *Vertebrate Limb and Somite Morphogenesis*, D. A. Ede, J. R. Hinchliffe, M. Balls, Eds. (Cambridge Univ. Press, Cambridge, 1977), p. 181.
2. S. R. Dienstman, J. Biehler, S. Holtzer, H. Holtzer, *Dev. Biol.* **39**, 63 (1974).
3. A. Caplan, *Exp. Cell Res.* **62**, 341 (1970); B. K. Hall, *Developmental and Cellular Skeletal Biology* (Academic Press, New York, 1978).
4. B. P. Toole, G. Jackson, J. Gross, *Proc. Natl. Acad. Sci. U.S.A.* **69**, 1384 (1972).
5. C. A. Lewis, R. M. Pratt, J. P. Pennyacker, J. R. Hassell, *Dev. Biol.* **64**, 31 (1978).
6. J. W. Saunders, Jr., *J. Exp. Zool.* **108**, 363 (1948).
7. \_\_\_\_\_ and M. T. Gasseling, in *Epithelial-Mesenchymal Interactions*, R. Fleischmajer and R. E. Billingham, Eds. (Williams & Wilkins, Baltimore, 1968), p. 78.
8. R. J. Stark and R. L. Searls, *Dev. Biol.* **33**, 138 (1973).
9. J. Lewis, *J. Embryol. Exp. Morphol.* **33**, 419 (1975).
10. D. Summerbell, *ibid.* **35**, 241 (1976).
11. J. W. Saunders, Jr., in *Vertebrate Limb and Somite Morphogenesis*, D. A. Ede, J. R. Hinchliffe, M. Balls, Eds. (Cambridge Univ. Press, Cambridge, 1977), p. 1.
12. R. L. Searls, *Dev. Biol.* **11**, 155 (1965).
13. \_\_\_\_\_, S. R. Hilfer, S. M. Mirow, *ibid.* **28**, 123 (1972).
14. P. V. Thorogood and J. R. Hinchliffe, *J. Embryol. Exp. Morphol.* **33**, 581 (1975).
15. S. Haushka and C. Haney, *J. Cell Biol.* **79**, 24a (1978); poster presentation, American Society for Cell Biology meeting, San Antonio, Tex., 1978.
16. P. B. Ahrens, M. Solursh, R. S. Reiter, C. T. Singley, *Dev. Biol.* **69**, 436 (1979).
17. B. Christ, H. J. Jacob, M. Jacob, *Anat. Embryol.* **150**, 171 (1977).
18. A. Chevallier, M. Kieny, A. Mauger, *J. Embryol. Exp. Morphol.* **41**, 245 (1977).
19. J. W. Saunders, Jr., and J. F. Fallon, in *Current Status of Some Major Problems in Developmental Biology, 25th Symposium of the Society of Developmental Biology*, M. Locke, Ed. (Academic Press, New York, 1967), p. 289; S. A. Newman, in preparation.
20. H. B. Fell and R. G. Canti, *Proc. R. Soc. London Ser. B* **116**, 316 (1934).
21. M. Solursh and R. S. Reiter, *Cell Differ.* **4**, 131 (1975); M. Solursh, P. B. Ahrens, R. S. Reiter, *In Vitro* **14**, 51 (1978).
22. A. M. Turing, *Philos. Trans. R. Soc. London Ser. B* **237**, 32 (1952).
23. S. A. Kauffman, R. M. Shymko, K. Trabert, *Science* **199**, 259 (1978).
24. D. S. Dawd and J. R. Hinchliffe, *J. Embryol. Exp. Morphol.* **26**, 401 (1971).
25. J. Tomasek and S. Newman, in preparation.
26. D. Summerbell, J. H. Lewis, L. Wolpert, *Nature (London)* **244**, 492 (1973).
27. J. W. Saunders, Jr., M. T. Gasseling, Sr., M. D. Gfeller, *J. Exp. Zool.* **137**, 39 (1958).
28. M. A. Napier and N. M. Hadler, *Proc. Natl. Acad. Sci. U.S.A.* **75**, 2261 (1978).
29. A. Vaheri, E. Ruoslahti, D. Mosher, Eds., *Fibroblast Surface Protein* (New York Academy of Sciences, New York, 1978); K. M. Yamada and K. Olden, *Nature (London)* **275**, 179 (1978).
30. W. J. Moore, *Physical Chemistry* (Prentice-Hall, Englewood Cliffs, N.J., ed. 3, 1963), p. 766.
31. The possibility that hyaluronate could play the role of our parameter  $I$  was suggested to us by J. Tomasek.
32. B. P. Toole, *Dev. Biol.* **29**, 321 (1972).
33. V. Hamburger and H. L. Hamilton, *J. Morphol.* **88**, 49 (1951).
34. Of course, the value we have used for  $S$  is an approximation. However, because of the form of Eq. 5,  $S$  can vary between 1 and 9 with relatively small changes (30 percent or less) in the chamber sizes in which appropriate numbers of the skeletal elements are produced. Small adjustments in the value of  $\lambda$  can easily compensate for these changes. The proximodistal progression of the emergence of rows of elements of increasing number remains unaltered.
35. L. Rubin and J. W. Saunders, Jr., *Dev. Biol.* **28**, 94 (1972).
36. U. K. Abbott, L. W. Taylor, H. Abplanalp, *J. Hered.* **51**, 195 (1960); R. Niederman and P. B. Armstrong, *J. Exp. Zool.* **181**, 17 (1972).
37. J. M. Cairns, in *Vertebrate Limb and Somite Morphogenesis*, D. A. Ede, J. R. Hinchliffe, M. Balls, Eds. (Cambridge Univ. Press, Cambridge, 1977), p. 123.
38. P. F. Goetinck and U. K. Abbott, *J. Exp. Zool.* **155**, 161 (1964).
39. J. R. Hinchliffe and D. A. Ede, *J. Embryol. Exp. Morphol.* **17**, 385 (1967).
40. D. A. Ede and G. S. Agerback, *ibid.* **20**, 81 (1968); D. A. Ede and O. P. Flint, *J. Cell Sci.* **18**, 97 (1975); *ibid.*, p. 301; D. A. Ede, in *The Cell Surface in Animal Embryogenesis and Development*, G. Poste and G. Nicolson, Eds. (North-Holland, Amsterdam, 1977), p. 495.
41. M. A. Perle and S. Newman, in preparation.
42. Model calculations with Eq. 9, experimental values for  $l_y$  in *talpid<sup>2</sup>*, and normal values for the other parameters give rise to patterns of "chondrogenesis" corresponding to those observed in the mutant.
43. A. J. T. Millis and M. Hoyle, *Nature (London)* **271**, 668 (1978).
44. L. B. Chen, A. Murray, R. A. Segal, A. Bushnell, M. L. Walsh, *Cell* **14**, 377 (1978).
45. R. R. Markwald, T. P. Fitzharris, H. Bank, D. H. Beranke, *Dev. Biol.* **62**, 292 (1978).
46. J. Tomasek and S. A. Newman, *J. Cell Biol.* **79**, 153a (1978).
47. L. B. Chen, *Cell* **10**, 393 (1977).
48. M. Kieny, in *Vertebrate Limb and Somite Morphogenesis*, D. A. Ede, J. R. Hinchliffe, M. Balls, Eds. (Cambridge Univ. Press, Cambridge, 1977), p. 87.
49. J. R. Hinchliffe, *ibid.*, p. 293.
50. D. Summerbell and C. Tickle, *ibid.*, p. 24; C. Tickle, D. Summerbell, L. Wolpert, *Nature (London)* **254**, 199 (1975).
51. O. K. Wilby and D. A. Ede, *J. Theor. Biol.* **52**, 199 (1975).
52. V. French, P. Bryant, S. V. Bryant, *Science* **193**, 969 (1976).
53. F. H. Swett, *J. Exp. Zool.* **44**, 419 (1926); D. L. Stocum, *Differentiation* **3**, 167 (1975); L. E. Iten and S. V. Bryant, *Dev. Biol.* **44**, 119 (1975); M. Maden, *J. Theor. Biol.* **69**, 735 (1977); J. M. W. Slack and S. Savage, *Cell* **14**, 1 (1978). An interesting model that generates a realistic limb skeletal pattern under an entirely different set of assumptions from ours has been presented by H. K. MacWilliams and S. Papageorgiou [*J. Theor. Biol.* **72**, 385 (1978)].
54. Note that we present no theory of the origin of the limb apex as a morphogenetically active structure. That process is presumed to occur on the plane of the flank before the initiation of limb outgrowth.
55. The processes by which  $M$  is absorbed at the limb periphery can include the formation of feather germs, scales, and other integumentary structures. In our simple model the boundary conditions for the concentration of  $M$  are circumferentially uniform. If actual nonuniformities in the integument [J. W. Saunders, Jr., and M. T. Gasseling, *J. Exp. Zool.* **135**, 503 (1975); P. Sengel, *Ciba Found. Symp.* **29**, 51 (1975)] were reflected in nonuniformities in the boundary conditions for Eq. 1, a means would be available for encoding the anteroposterior and dorsoventral asymmetries of the skeleton at the limb periphery, as suggested by the experiments of R. J. Stark and R. L. Searls [*Dev. Biol.* **38**, 51 (1974)] and the analysis of French et al. (52).
56. We have no a priori way of determining the sign of  $r$  (Eq. A3) since it depends on the detailed form of the biosynthetic rate function  $R$ , which we have not presented. Furthermore, since we have not assumed that the initial spatially homogeneous state  $C = C_0$  is time-independent, there is no reason to expect  $r$ , as defined in Eq. A3, to represent the usual first-order biosynthetic decay constant: an  $r$  of either sign would be physically reasonable. If we set  $S$  (Eq. 5) at roughly  $-6$  (assuming a negative  $r$ ), we are required to set  $\lambda$  at  $7/d$  in order to form a single element in a diffusion chamber 0.7 mm long. This provides for a greater than 1000-fold differential in the extreme values of  $c$ , as compared with the less than 100-fold differential that arises under the assumption of a positive  $r$ . Transitions to two and three elements occur in chambers of length 0.6 and 0.47 mm, respectively, when  $r$  is taken as negative. This does not correspond as well as with observed values as does the positive case. For these reasons, we suggest that if skeletal pattern formation is in fact governed by processes similar to those outlined here, the actual biosynthetic rate function will be such as to give a positive  $r$ .
57. Our mathematical formulation does not include a description of the complete, time-dependent behavior of the system we have modeled. As a result, we cannot rigorously establish the emergence of the first or any successive stationary state of the system from mathematical first principles, although we consider our analysis plausible. Similar considerations hold for the stability of our solutions to small perturbations [see J. Bard and I. Lauder, *J. Theor. Biol.* **45**, 501 (1974)], which in any case depends on the detailed form of the biosynthetic rate function  $R(c)$ , which is unknown at present. Possibly unstable transients in  $c$  between the steady states in successive chambers of fixed size are avoided by use of the parameter  $I$ , as described in the text.
58. We are grateful to J. W. Saunders, Jr., for advice and encouragement during all stages of this work. We thank J. Percus, J. Keller, C. Peskin, and S. Childress of the Courant Institute, New York, for their comments on an earlier version of the model. We also thank J. Tomasek for valuable suggestions, N. Seeman and S. Greenstein for help with the computer graphics, R. Loos for the line drawings, and L. Callahan for preparing the typescript. Supported in part by NSF grant CHE 76-82583A01 to H.L.F. and NIH grant GM26198-01 to S.A.N.